Progr Colloid Polym Sci (1998) 111:41–47

Z. Adamczyk
B. Siwek
P. Weronski
M. Zembala

Adsorption of colloid particle mixtures at interfaces

Z. Adamczyk (✉) · B. Siwek
P. Weronski · M. Zembala
Institute of Catalysis and Surface Chemistry
Polish Academy of Sciences
30-239 Cracow, Niezapominajek 1
Poland

Abstract Adsorption of polydisperse colloid mixtures, including the limiting case of adsorption at surfaces precovered with smaller sized particles, was studied theoretically and experimentally. The theoretical analysis of these phenomena was carried out using the generalized random sequential adsorption (RSA) model suitable for irreversible systems. In order to determine the range of applicability of the RSA model for reversible systems, numerical simulations were compared with the analytical results stemming from the equilibrium scaled particle theory. Some theoretical predictions concerning adsorption at precovered surfaces and adsorption of bimodal mixtures were discussed, i.e., the blocking functions, the kinetics and the jamming coverages. These theoretical predictions were compared with experimental data obtained for model latex suspensions using the direct microscope observation method combined with the impinging jet technique. Adsorption kinetics at the mica surface precovered with smaller particles was studied as well as adsorption from bimodal mixtures of particles differing widely in size. The characteristic features of the RSA models were quantitatively confirmed in these experiments which supported the hypothesis that small colloid particles, polymer or surfactants present in trace amounts may significantly reduce adsorption rates of larger particles.

Key words Adsorption of colloids – colloid adsorption – kinetics of colloid adsorption – structure of adsorbed colloids

Introduction

Adsorption of colloid and bioparticles is of a large practical significance for polymer and colloid science, biophysics and medicine enabling a better control of colloid, protein and cell separation processes (e.g., by filtration, chromatography), enzyme immobilization, thrombosis, biofouling of transplants and artificial organs, etc. Often in these processes, especially in filtration, polydisperse suspensions or mixtures occur, e.g., colloid/polymer, colloid/macroscopic particle or protein/surfactant. Due to their higher diffusivity and number concentration the smaller particles or molecules will first adsorb at the interface forming a layer which may prevent adsorption of larger particles. Thus, the competition from the mobile component will result in "poisoning" of interfaces before an appreciable accumulation of larger particles takes place as reported often in the literature [1–3]. Similar problems appear in model experiments concerning particle or protein adsorption when the usual cleaning procedure may produce a layer of contamination at the substrate surface difficult to detect. This is

expected to affect adsorption kinetics in the proper experiments. Hence the problem of polydisperse mixture adsorption seems important from a practical viewpoint considering the fact that few systematic studies were carried out on this subject, either theoretical or experimental.

Thus, the goal of our present work was to develop theoretical models for a quantitative analysis of kinetic and structural aspects of polydisperse mixture adsorption. In view of the complexity of the problem we confined our experiments to bimodal suspensions composed of smaller sized and larger sized monodisperse polystyrene latex suspensions mixed at various concentration ratios. As a reference state we also consider the practically important situation of larger particle adsorption at surfaces precovered with a given amount of smaller particles.

The theoretical approaches

The RSA simulation method

Polydisperse mixture adsorption, including the limiting case of adsorption at precovered surfaces, was analyzed theoretically in terms of the random sequential adsorption (RSA) method which is one of the simplest and most efficient approach to analyze sequences of irreversible events [4–7]. In this process particles are placed randomly, one upon a time, over a plane of isotropic properties. Once an empty space element is found the particle becomes irreversibly adsorbed (with no consecutive motion allowed). Otherwise it is rejected and a new addition attempt is undertaken totally uncorrelated with previous attempts. The process usually starts from an empty plane and continues until the jamming state when no additional object can be introduced to the volume.

The simulation algorithm used in our work was similar to that used for polydisperse sphere adsorption described in [8]. The simulations were carried out over a square of unit length with the usual periodic boundary conditions at its perimeter. A subsidiary matrix was introduced in order to facilitate the overlapping test. Particle positions and size distributions (e.g. Gaussian, uniform or bimodal) were simulated by using the high-quality pseudo-random number generator as described in [6, 8].

Adsorption of larger particles at surfaces precovered with smaller sized particles was simulated using the algorithm consisting of the two main stages:

(i) first the simulation plane was covered with smaller sized particles to a prescribed dimensionless surface concentration (coverage) $\theta_s = \pi a_s^2 N_s$ (where a_s is the radius of these particles and N_s is the surface concentration of smaller particles); during this stage the usual RSA simulation algorithm was used [8],

(ii) then, the larger spheres having the radius a_l were adsorbed by choosing at random their position within the simulation area; the overlapping test between larger/larger and smaller/larger particle pairs was carried out by considering the true three-dimensional distances between the sphere centers.

In order to simulate the kinetic runs the dimensionless adsorption time τ was defined as

$$\tau = \frac{N_{att}}{N_{ch}}, \tag{1}$$

Where N_{att} is the overall number of attempts to place particles and N_{ch} is the characteristic surface concentration.

The surface blocking parameter B (also called the available surface function ASF) for larger particles was calculated according to the method of Schaaf and Talbot [5] by exploiting the definition

$$B = \frac{p(\theta_s, \theta_l)}{p_0} = \frac{N_{succ}}{N_{att}}, \tag{2}$$

where p is the probability of adsorbing the larger particle at the surface characterized by the coverages θ_s, $\theta_l = \pi a_l^2 N_l$ (N_l is the surface concentration of larger particles) and p_0 is the probability of adsorption at uncovered surface (assumed equal to one without loss of generality) and N_{succ} is the number of successful adsorption events performed at fixed θ_s, θ_l. In practice, N_{att} was about 10^6 in order to attain a sufficient accuracy of B.

The analytical approximations

Adsorption kinetics of a bimodal mixture of spherical particles is governed by the system of two coupled surface mass balance equations [9]

$$\frac{d\theta_s}{dt} = \pi a_s^2 \bar{j}_s^0 n_s B_s(\theta_l, \theta_s),$$

$$\frac{d\theta_l}{dt} = \pi a_l^2 \bar{j}_l^0 n_l B_l(\theta_l, \theta_s), \tag{3}$$

where $\bar{j}_l^0$, $\bar{j}_s^0$ are the reduced initial fluxes (for uncovered surfaces) of larger and smaller particles, respectively and B_l, B_s are the surface blocking parameters for larger and smaller particles, respectively.

Equation (3) can be expressed in a more concise, dimensionless form as

$$\frac{d\theta_s}{d\tau} = \frac{K_s}{K_s + \lambda^2} B_s(\theta_l, \theta_s),$$

$$\frac{d\theta_l}{d\tau} = \frac{\lambda^2}{K_s + \lambda^2} B_l(\theta_l, \theta_s), \tag{4}$$

where $\tau = \pi a_1^2 \bar{j}_1^0 n_1 (1 + (K_s/\lambda^2))t$ is the dimensionless time, $\lambda = a_l/a_s$ is the particle size ratio and $K_s = \bar{j}_s^0 n_s / \bar{j}_1^0 n_l$ is the dimensionless adsorption constant of smaller particles.

Equation (4) can be integrated by standard methods when analytical expressions for B_s and B_l are known. As mentioned above, in the case of irreversible adsorption governed by RSA model these blocking functions can only be derived from numerical simulations. However, useful analytical approximations for B_s and B_l can be obtained by exploiting the scaled particle theory (SPT) formulated in [10] for disks and disk mixtures [11, 12] and extended later on for sphere adsorption [14]. These functions are explicitly given by the expressions

$$B_s = (1 - \theta)\, e^{-\left[\frac{3\theta_s + (\frac{4}{\lambda} - 1)\theta_l}{1-\theta} + \left(\frac{\theta_s + (\frac{2}{\sqrt{\lambda}} - 1)\theta_l}{1-\theta}\right)^2\right]},$$

$$B_l = (1 - \theta)\, e^{-\left[\frac{3\theta_l + (4\lambda - 1)\theta_l}{1-\theta} + \left(\frac{\theta_l + (2\sqrt{\lambda} - 1)\theta_s}{1-\theta}\right)^2\right]}, \quad (5)$$

where $\theta = \theta_s + \theta_l$.

It is interesting to note that the low coverage expansion of B_l in the case of absorption at precovered surfaces assumes the form

$$B_l = 1 - C_1(\theta_s)\theta_l = 1 - \frac{\theta_l}{\theta_{mx}}. \quad (6)$$

Hence, a quasi-Langmuirian behavior is predicted with θ_{mx} given by the expression [14]

$$\theta_{mx} \cong \frac{1}{4 + (4\lambda + 4\sqrt{\lambda} - 7)\theta_s}. \quad (7)$$

In the general case the θ_l or θ_s vs. τ dependencies were obtained by integrating Eq. (4) by the Runge–Kutta method.

Experimental procedure

The experimental setup described in detail in our previous works [3, 8, 13] was based on the circular impinging-jet principle and direct in situ microscope observations of particle adsorption. Since the size of the particle was close to a micrometer we were able to determine in real time the surface concentration (number of particles adsorbed over a given surface) of both small and large particles. We used the freshly cleaved mica sheets as the substrate. In the case where negatively charged colloid mixtures were used the negative surface charge of mica was converted into a positive one due to the irreversible adsorption of Al^{3+} salts in a procedure similar to that previously described [13].

The latex suspensions were produced in a surfactant-free polymerization procedure with the persulfate initiator in case of negative particles and a special azonitrile initiator for the positive ones [3]. In this study we used two monodisperse latex samples (i) characterized by the averaged size determined by the Coulter–Counter to be $2a_l = 1.48 \pm 0.1$ μm (hereafter referred to as larger particles) and (ii) $2a_s = 0.68 \pm 0.05$ μm (referred to as smaller particles). Their size ratio a_l/a_s was, therefore, equal to 2.2. We also used a similar combination of positively charged latices having the size $2a_l = 1.12 \pm 0.1$ and $2a_s = 0.55 \pm 0.05$ μm, respectively, characterized by $\lambda = 2.0$.

The ionic strength in these experiments was kept at 10^{-4} M (by addition of recrystallized KCl solution) and the pH was about 6.0. The volume velocity of the suspension Q was equal to 0.009 cm^3/s, which corresponded to Reynolds number of 4, or 0.018 cm^3/s for $Re = 8$.

The experimental procedure described in detail in our previous works [3, 13] consisted in provoking the suspension motion through the cell at a fixed rate (due to hydrostatic pressure difference between the suspension container and the cell outlet tube). Then, the number of particles adsorbing over areas close to the center of the cell (in order to minimize the hydrodynamic scattering effects) was recorded in real time using image processing. The initial fluxes of monodisperse suspensions were determined in separate experiments by differentiating a polynomial which fitted best the initial kinetic date, i.e., the coverage vs. time dependencies.

In the case of adsorption at precovered surfaces the experimental procedure was slightly different: first the smaller particles were adsorbed at the mica surface under the usual procedure [3, 13] until a given coverage θ_s was attained. In our experiments θ_s varied between 0 (uncovered surface) to 30%. Then the small particle suspension was replaced in situ by the larger particle suspension characterized by the bulk number concentration n_b. A short transition time (of the order of 1 min) was allowed before the proper adsorption experiments of larger particles were recorded.

Results and discussion

The theoretical predictions

Using the RSA numerical algorithm described above one can determine not only the blocking functions of small and large particles and their adsorption kinetics but also the jamming coverages and the structure of the adsorbed layers at transient and jammed states.

The quantity of considerable practical interest is the $B_l^0(\theta_s)$ function which represents the averaged probability of adsorbing a particle over a surface precovered by smaller particles (coverage θ_s) normalized to the probability of adsorbing the particle over an uncovered surface. Thus, by

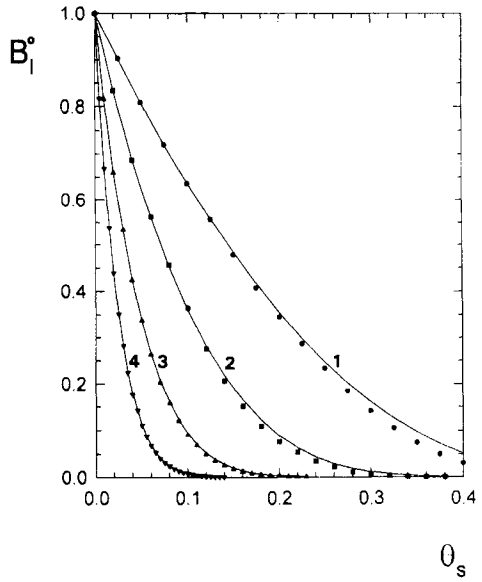

Fig. 1 The dependence of B_1^0 on the surface concentration of smaller particles θ_s. The points denote numerical simulations performed for: (1) $\lambda = 1$ (reference, monodisperse system), (2) $\lambda = 2.2$, (3) $\lambda = 5$, (4) $\lambda = 10$, the continuous lines denote the equilibrium SPT results calculated from Eq. (5)

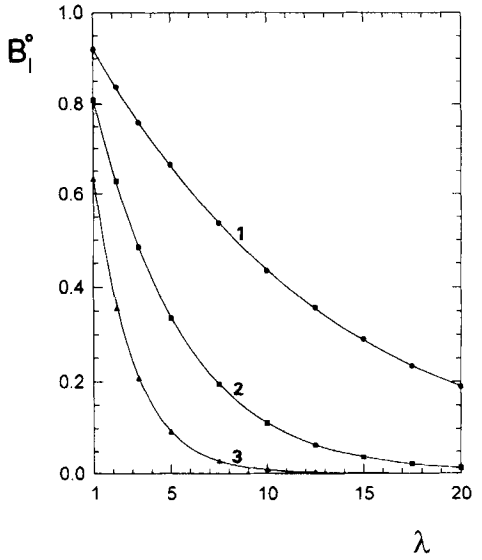

Fig. 2 The dependence of B_1^0 function of larger particles (normalized initial flux) on $\lambda = a_1/a_s$ determined numerically for: (1) $\theta_s = 2\%$, (2) $\theta_s = 5\%$, (3) $\theta_s = 10\%$, the continuous lines denote the equilibrium SPT results calculated from Eq. (5)

knowing B_1^0 one can calculate the initial flux (and hence adsorption kinetics for initial stages) at covered surfaces from the simple relationship

$$\bar{j} = \bar{j}_1^0 B_1^0(\theta_s) \,. \tag{8}$$

In Fig. 1 the dependence of B_1^0 on θ_s is plotted for $\lambda = 1$ (reference curve for monodisperse spheres), 2.2, 5 and 10, respectively. As can be noticed, adsorption probability of larger particles is considerably decreased by the presence of adsorbed small particles, especially for higher λ values. It is interesting to note that the analytical SPT results represented by Eq. (5) (when the value $\theta_1 = 0$ is substituted) reflect well the characteristic features of the B_1^0 function, especially its fast, quasi-exponential decrease for higher coverages. The agreement between the RSA simulations and these analytical predictions seems quantitative when $B_1^0 > 0.1$. As expected the deviation between equilibrium and RSA results are increased for higher θ_s values when B_1^0 became considerably smaller than 0.1

It seems therefore, in view of the limited experimental accuracy, especially for higher coverages of smaller particles, that the SPT results can be used for practical purposes as a good estimate of B_1^0 (initial flux) on precovered surfaces.

The results shown in Fig. 1 also suggest that the presence of small amounts of smaller particles, e.g., of the colloid type should result in a significant decrease in adsorption of larger particles. This "surface poisoning" effect is further illustrated by the data shown in Fig. 2. As one can see the value of B_1^0 decreased abruptly, for a fixed θ_s as the size of the preadsorbed particles is decreased.

The kinetic curves, i.e., the θ_1 vs. τ dependencies derived from the numerical RSA-type simulations for $\lambda = 10$ and various surface concentrations of smaller particles θ_s are shown in Fig. 3. For comparison, the analytical results calculated by integrating Eq. (4) with the blocking function described by the quasi-Langmuirian model, Eq. (6), are also shown. As can be seen, as this model gives for θ_1 the explicit expression

$$\theta_1 = \theta_{mx}[1 - e^{-B_1^0 \tau/\theta_{mx}}] \,, \tag{9}$$

it can be used as a reasonable estimate of adsorption kinetics on precovered surfaces, especially for higher coverages θ_s.

It should be noted, however, that for a very long adsorption time, $\tau \gg 4$, considerable deviations from the quasi-Langmuirian model appear (see Fig. 3) and the adsorption regime is changed. It can be then better described by the power law approach at the saturation (jamming) concentration which is characteristic for many RSA processes [3, 7]

$$\theta_1^\infty - \theta_1 \sim \tau^{-1/2} \,, \tag{10}$$

where $\theta_1^\infty(\theta_s)$ is the jamming coverage of larger particles at surfaces precovered with a given amount of smaller particles.

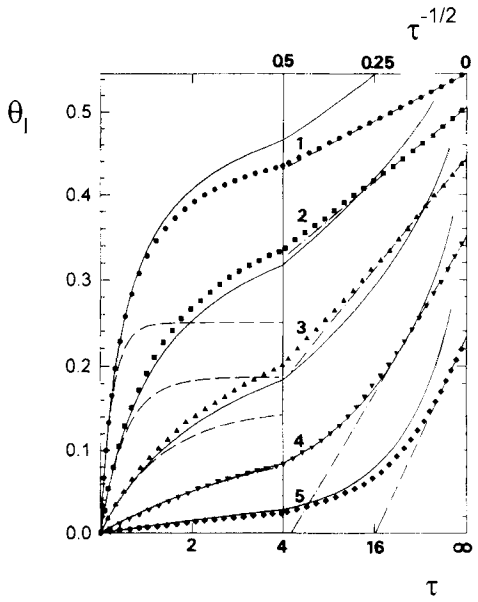

Fig. 3 Kinetics of larger particle adsorption at surfaces precovered with smaller particles (numerical RSA simulations) expressed as θ_1 vs. τ dependence, $\lambda = 10$: (1) $\theta_s = 0\%$, (2) $\theta_s = 2.5\%$, (3) $\theta_s = 5\%$, (4) $\theta_s = 7\%$, (5) $\theta_s = 10\%$, the continuous lines denote the SPT equilibrium results, the broken lines show the analytical results calculated from Eq. (9) and the (· ·–·) lines denoted the linear fits

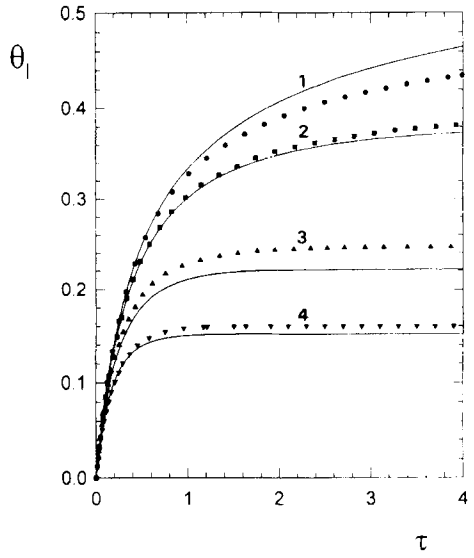

Fig. 4 Kinetics of bimodal sphere adsorption derived from RSA simulations for $\lambda = 10$: (1) $K_s = 0$ (monodisperse reference system), (2) $K_s = 1$, (3) $K_s = 5$, (4) $K_s = 10$, the continuous lines denote the analytical results obtained by numerical integration of Eq. (4)

It can be demonstrated [5, 14] that the θ_1 vs. $\tau^{-1/2}$ dependence implies that the ASF function for this asymptotic regime should assume the form

$$B_1 \sim [\theta_1^{\infty}(\theta_s) - \theta_1]^3 , \qquad (11)$$

where the jamming coverages θ_1^{∞} are dependent on the initial coverage of smaller particles.

The dependencies of these jamming concentrations θ_1^{∞} on θ_s obtained for various λ values are reported elsewhere [14]. Generally speaking, the jamming coverages of large particles are considerably reduced by the presence of particles whose size is considerably smaller, $\lambda > 5$ (e.g., colloids).

Similar effects as these discussed above for precovered surfaces also occur for bimodal mixture adsorption when the dimensionless adsorption rate K_s of the smaller component becomes larger than unity. This is illustrated well in Fig. 4 where the kinetic runs are shown for $\lambda = 10$. As can be observed fast adsorption of the smaller component from the mixture blocked adsorption of larger particles whose surface coverage was saturated at a very low value. However, in contrast to the case of preadsorbed surfaces, the θ_1 values drift little with time (for $\lambda > 5$) so the θ_1^{∞} values were consequently much smaller. One may draw, therefore, the conclusion that the surface poisoning effect becomes more pronounced for mixtures in comparison with precovered surfaces.

Adsorption at precovered surfaces or from bimodal mixtures differs also significantly in respect to structural aspects. For lack of space these interesting problems are discussed elsewhere [14].

Experimental evidences

The experimentally determined adsorption kinetics of large particles at surfaces precovered with a given amount of smaller particles is shown in Fig. 5. As one can notice, the increase in θ_s resulted in a considerable decrease in adsorption rate of larger particles so the surface coverages θ_1 attained after a long time in the presence of preadsorbed smaller particles became much lower than for uncovered surfaces.

The experimental kinetic runs were compared with the RSA simulations performed according to the procedure described above (solid lines in Fig. 5). As one can notice, the experimental results are well accounted for by the RSA model with electrostatic interactions neglected (hard particle limit). This can be explained by the relatively high ionic strength and rather low surface concentration of larger particles, so the electrostatic interactions became effectively screened [15].

The analytical predictions stemming from the quasi-Langmuir model (Eq. (6)) are also plotted in Fig. 5 (dotted lines). As can be seen they are in a good agreement with the numerical simulations and experimental results for the

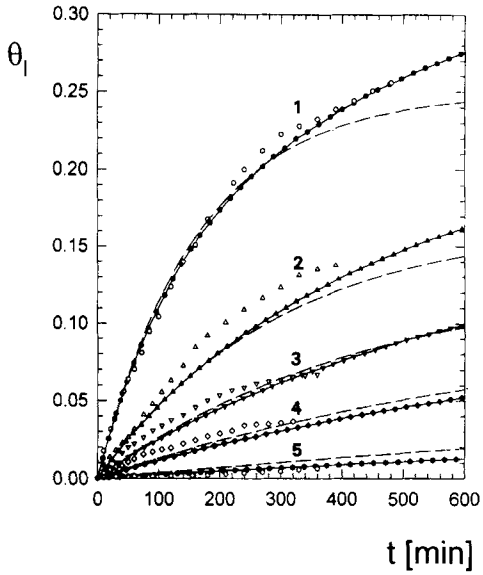

Fig. 5 Kinetics of polystyrene particle adsorption ($2a_l = 1.48\ \mu m$) at mica surface precovered by various amounts of smaller particles ($2a_s = 0.68\ \mu m$): (1) $\theta_s = 0$ (uncovered surface), (2) $\theta_s = 10\%$, (3) $\theta_s = 15\%$, (4) $\theta_s = 20.5\%$, (5) $\theta_s = 27\%$, the empty points denote the experimental results, the full symbols denote the RSA simulations, the broken lines represent the quasi-Langmuir model Eq. (9)

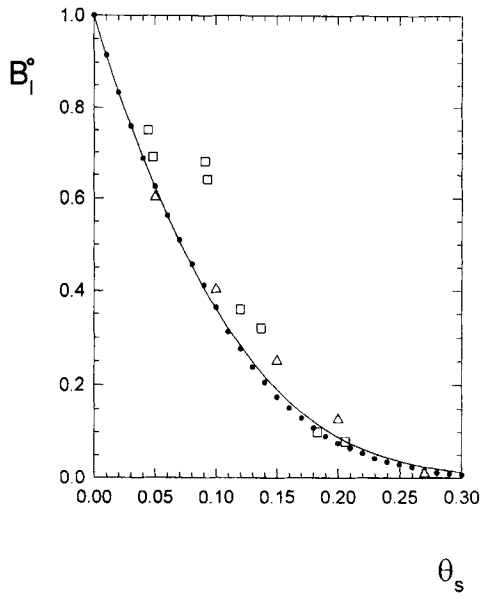

Fig. 6 The dependence of the reduced initial flux B_l^0 of larger particles at the mica surface covered by smaller particles; the triangles and squares denote the experimental results obtained for negative and positive particles, respectively, the circles denote the theoretical results derived from the RSA simulations and the continuous line respresents the SPT results

entire range of θ, especially for shorter adsorption times ($t < 300$ min).

It should also be noted in Fig. 5 that for longer adsorption times ($t > 300$ min) the kinetic curves seem to approach stationary (saturation) values of θ. This is, however, an apparent saturation effect because from the numerical predictions discussed above one can deduce that the true limiting values of θ are much higher. However, the physical adsorption time needed to approach the true jamming limits becomes excessively long, especially for higher θ_s values (of the order of days for the bulk suspension concentration equal 4×10^8 cm^{-3}). For such long-lasting experiments, however, the chances of contaminating the system are increased which makes them less reliable.

Therefore, the kinetic runs as these shown in Fig. 5 are not suitable for determining the maximum surface coverages. They can be used, however, with a good accuracy to derive the initial flux at covered surfaces.

The results are shown in Fig. 6 in the form of the dependence of the reduced flux $\bar{j}_l/\bar{j}_l^0 = B_l^0$ on θ_s (where the initial flux at uncovered surfaces $\bar{j}_l^0$ was determined in separate experiments). This quantity can be treated as the blocking parameter of larger particles at surfaces precovered by small particles. As can be seen in Fig. 6 the experimental results (obtained both for negatively and positively charged particles) can well be described by the numerical RSA simulations. Also, the analytical expressions stemming from the equilibrium SPT theory are in good agreement with our experimental results which demonstrated that the presence of smaller particles exerted a profound effect on adsorption of larger particles. The initial flux for θ_s as low as 10% was found almost three times smaller than for clean surfaces. For θ_s equal to 20%, the initial flux at precovered surfaces is reduced by more than 10 times.

It should be mentioned that the effects measured in our work which are stemming from the surface exclusions effects exceed by orders of magnitude the effects predicted theoretically by Dabroś and van de Ven [16] originating from hydrodynamic corrections due to the presence of adsorbed particles.

Similar effects were observed in the case of polydisperse mixture adsorption as shown in Figs. 7 and 8. One can see that the presence of small particles in the mixture significantly decreases the adsorption kinetics of larger particles whose maximum surface coverage saturated at very small values, especially for $K_s > 1$ (cf. Fig. 8). Similarly, for precovered surfaces the appearance of the poisoning effect of smaller particles was, therefore, spectacularly demonstrated. It should be noted that the experimental results shown in Figs. 7 and 8 can well be interpreted in terms of the RSA simulations and the analytical SPT results (derived by numerical integration of Eq. (4)).

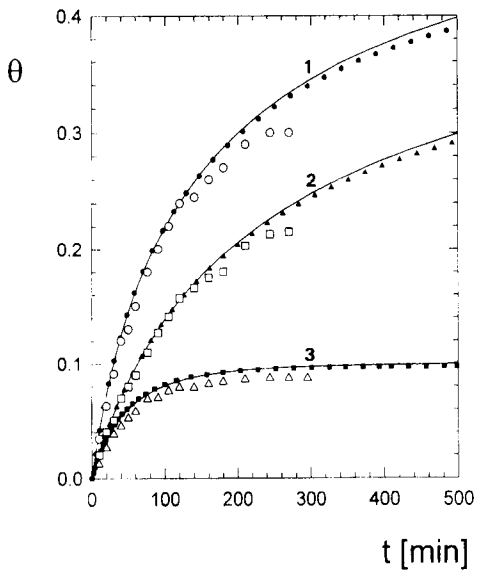

Fig. 7 Kinetics of adsorption from bimodal mixtures, $\lambda = 2.2$, $K_s = 5$; the empty symbols show the experimental results obtained for latex particles, the full symbols show the RSA numerical results and the continuous lines represent the SPT results: (1) $\theta_l + \theta_s$, (2) θ_s, (3) θ_l

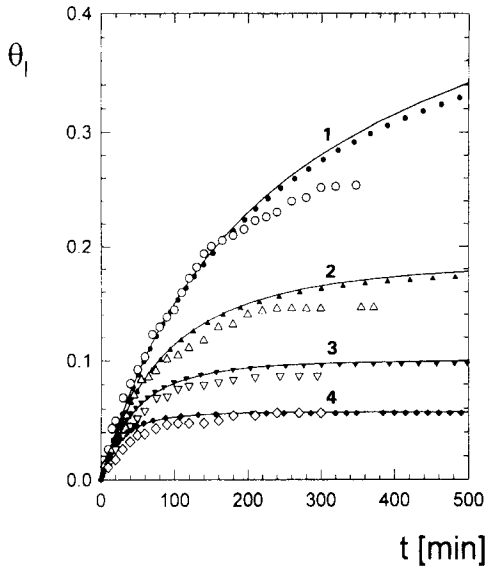

Fig. 8 Kinetics of larger particle adsorption from bimodal mixtures, $\lambda = 2.2$; the empty symbols show the experimental results obtained for: (1) $K_s = 0$ (monodisperse, reference system), (2) $K_s = 2$, (3) $K_s = 5$, (4) $K_s = 10$, the full symbols show the RSA results and the continuous lines represent the SPT results

The sensitivity of adsorption kinetics of larger particles to the presence of smaller particles (either at surfaces or in the bulk of the suspension) suggests that for suspensions contaminated with trace amounts of very small particles inaccurate results could be obtained resembling apparently Langmuirian-type kinetics.

Concluding remarks

It has been found that the numerical RSA simulations performed for bimodal sphere adsorption can well be approximated in the limit of low densities by the extrapolated SPT theory with the blocking functions given by Eq. (5).

These theoretical predictions and experimental results obtained for model suspensions suggest that both the adsorption kinetics (initial flux) and the jamming coverages of larger particles are very sensitive to the presence of trace amounts of smaller sized particles (colloids, polymers) at the interfaces, often difficult to detect by conventional analytical means. These theoretical predictions may explain the persisting difficulties in obtaining reliable kinetic data and monolayer densities in colloid protein adsorption processes.

Acknowledgements This work was partially supported by the KBN Grant: No 3T09 A08310.

References

1. Boluk MY, van de Ven TGM (1990) Colloids Surf 46:157–175
2. van de Ven TGM, Kelmen SJ (1996) J Colloid Interface Sci 181:118–123
3. Adamczyk Z, Siwek B, Zembala M, Belouschek P (1994) Adv Colloid Interface Sci 48:151–280
4. Hinrichsen EL, Feder J, Jossang T (1986) J Stat Phys 44:73–827
5. Schaaf P, Tablbot J (1989) J Chem Phys 91:4401–4408
6. Adamczyk Z, Weroński P (1996) J Chem Phys 105:5562–5573
7. Evans JW (1993) Rev Mod Phys 65:1281–1329
8. Adamczyk Z, Siwek B, Zembala M, Weroński P (1997) J Colloid Interface Sci 185:236–244
9. Talbot J, Schaaf P (1989) Phys Rev A 40:422–427
10. Reiss H, Frisch HL, Lebowitz JL (1959) J Chem Phys 31:369–380
11. Lebowitz JL, Helfand E, Preastgaard E (1965) J Chem Phys 43:774–779
12. Talbot J, Jin X, Wang NHL (1994) Langmuir 10:1663–1666
13. Adamczyk Z, Siwek B, Weroński P (1997) J Colloid Interface Sci 195: 261–263
14. Adamczyk Z, Weroński P (1997) J Chem Phys 108:9851–9858
15. Adamczyk Z, Warszyński P (1996) Adv Colloid Interface Sci 63:41–150
16. Dabroś T, van de Ven TGM (1993) Colloids Surf A 75:95–104